



Peer review status:

This is a non-peer-reviewed preprint submitted to EarthArXiv.

# A Multiscale Geometric PDE Framework Coupling Macroscopic Curvature and Microscopic Grain Boundary Motion: An Application to Snow Deformation and Sintering

Hiroshi Matsuda<sup>1\*</sup>, Shin'ichi Homma<sup>1</sup>

<sup>1</sup> Kokusai Kogyo Co., Ltd., 2-24-1, Harumi-cho, Fuchu-shi, Tokyo 183-0057, Japan

\* Corresponding author: hiroshi\_matsuda@kk-grp.jp

## Abstract

The motion of grain boundaries in polycrystalline materials and porous media has conventionally been modeled by local geometric evolution equations, such as Mean Curvature Flow (MCF). However, existing models primarily depend on local interfacial geometry and generally do not account for the influence of macroscopic curvature fields induced by the deformation of the bulk continuum. In this study, we propose a multiscale geometric continuum framework in which the macroscopic Gaussian curvature field modulates the evolution velocity of the microscopic MCF through a variationally motivated geometric driving term.

In our framework, for analytical clarity, the macroscopic continuum is restricted to a two-dimensional manifold. Its deviation from a stress-free state due to non-uniform deformation is described as the emergence of a nonzero Gaussian curvature field. Simultaneously, at the microscopic scale, the thermodynamic interface growth vector governed by the Laplace-Beltrami operator is formulated. This model integrates the dynamics of two distinct scales—the accumulation of strain energy due to macroscopic curvature and the microscopic topological changes (bonding and rupture of the grain boundary network)—into a single geometric evolution equation.

We discuss the mathematical well-posedness of the proposed coupled system, indicating local-in-time existence under bounded curvature assumptions ( $|K| < K_0$ ). As an illustrative application, the framework is applied to the macroscopic deformation and microscopic sintering process of snow, a porous material undergoing structural changes near its melting point. This geometric approach provides an analytical foundation for examining the mechanisms of fracture and topology changes in materials undergoing phase changes.

**Keywords:** Geometric Partial Differential Equations; Mean Curvature Flow; Multiscale Modeling; Variational Methods; Gaussian Curvature; Topology Change; Snow Deformation; Snow Sintering; Failure Initiation

## 1 Introduction

The evolution of interfaces and grain boundary motion in polycrystalline materials and porous media have been modeled using local geometric partial differential equations (PDEs), such as Mean Curvature Flow (MCF) and surface diffusion governed by the Laplace-Beltrami operator [4, 11]. While these classical models describe the smoothing and growth of microscopic structures, they rely on the local geometry of the interface [2]. Consequently, they often lack the capacity to account for the influence of macroscopic deformation applied to the bulk material and the resulting macroscopic curvature fields.

To address this limitation, we introduce a multiscale geometric PDE framework in which the curvature of a macroscopic manifold modulates the evolution velocity of a microscopic MCF. For analytical clarity, we restrict the present formulation to a two-dimensional manifold and describe the accumulation of strain energy induced by macroscopic deformation as the emergence of a nonzero Gaussian curvature field on the manifold. We show that this macroscopic curvature acts as an external geometric field that drives and affects the microscopic interface growth vector governed by the Laplace-Beltrami operator.

The mathematical structure of the proposed model differs from conventional generalizations of MCF. Specifically, we define a unified energy functional  $\mathcal{E}(\Omega, \Gamma)$  that integrates the microscopic surface free energy and the macroscopic elastic strain energy [5], expressed as:

$$\mathcal{E}(\Omega, \Gamma) = \int_{\Gamma} \gamma_0 dA + \epsilon \int_{\Omega} W_{\text{macro}}(K_{\text{macro}}) dV$$

where  $\Gamma$  is the microscopic interface,  $\Omega$  is the macroscopic bulk region, and  $\gamma_0$  is the surface tension. For simplicity, we assume that the accumulated macroscopic strain energy admits an effective geometric representation through a curvature-dependent density  $W_{\text{macro}}(K_{\text{macro}})$ .

By taking the first variation of this functional, we derive the coupled geometric evolution equation as an  $L^2$ -gradient flow, yielding a normal velocity  $V_n$  of the interface in the form:

$$V_n = -M(\gamma_0 H + \epsilon f(K_{\text{macro}}))$$

where  $M$  is the mobility,  $H$  is the mean curvature, and  $f(K_{\text{macro}})$  represents the variation of the macroscopic strain energy. In this framework, the macroscopic curvature tensor affects the microscopic topological changes—specifically, the formation and rupture of the grain boundary network. Furthermore, by introducing a parameter  $\epsilon \ll 1$  that characterizes the scale separation between the macroscopic bulk and the microscopic interfaces, the resulting problem naturally constitutes a singularly perturbed geometric evolution system, offering a mathematical structure for asymptotic analysis.

For the proposed coupled PDE system, we formulate sufficient conditions for the behavior of the solutions and state that local-in-time existence is established under the assumption of a bounded curvature field ( $|K_{\text{macro}}| < K_0$ ). By evaluating the conditions for topological changes (rupture of the interface), we provide an analytical foundation for the geometric framework.

As a representative example, snow is considered as a porous material exhibiting curvature-driven microstructural evolution near its melting point. The macroscopic deformation and failure of snow have conventionally been modeled using empirical approaches, which often struggle with the intractable complexity of its dynamic microstructural changes [7,9]. Consequently, the development of theoretical models tied to fundamental microscopic mechanisms has been widely recognized as a critical challenge [1,3,8,10]. By analyzing how our coupled PDE model represents the phenomena of macroscopic failure and microscopic ice-bonding dynamics, we explore the connection between geometric PDEs and the mechanical behavior of complex materials.

The principal contribution of this paper is the derivation of a new geometric evolution equation in which the velocity of a microscopic interface is coupled to a macroscopic curvature field through a variationally defined energy functional. The overall framework of this study is illustrated in Fig. 1. The remainder of this paper is organized as follows: Section 2 sets up the physical object and continuum model; Section 3 develops the macroscopic differential geometric formulation; Section 4 derives the coupled macroscopic-microscopic model via the variational principle; Section 5 presents an illustrative computational example; and Section 6 provides concluding remarks.

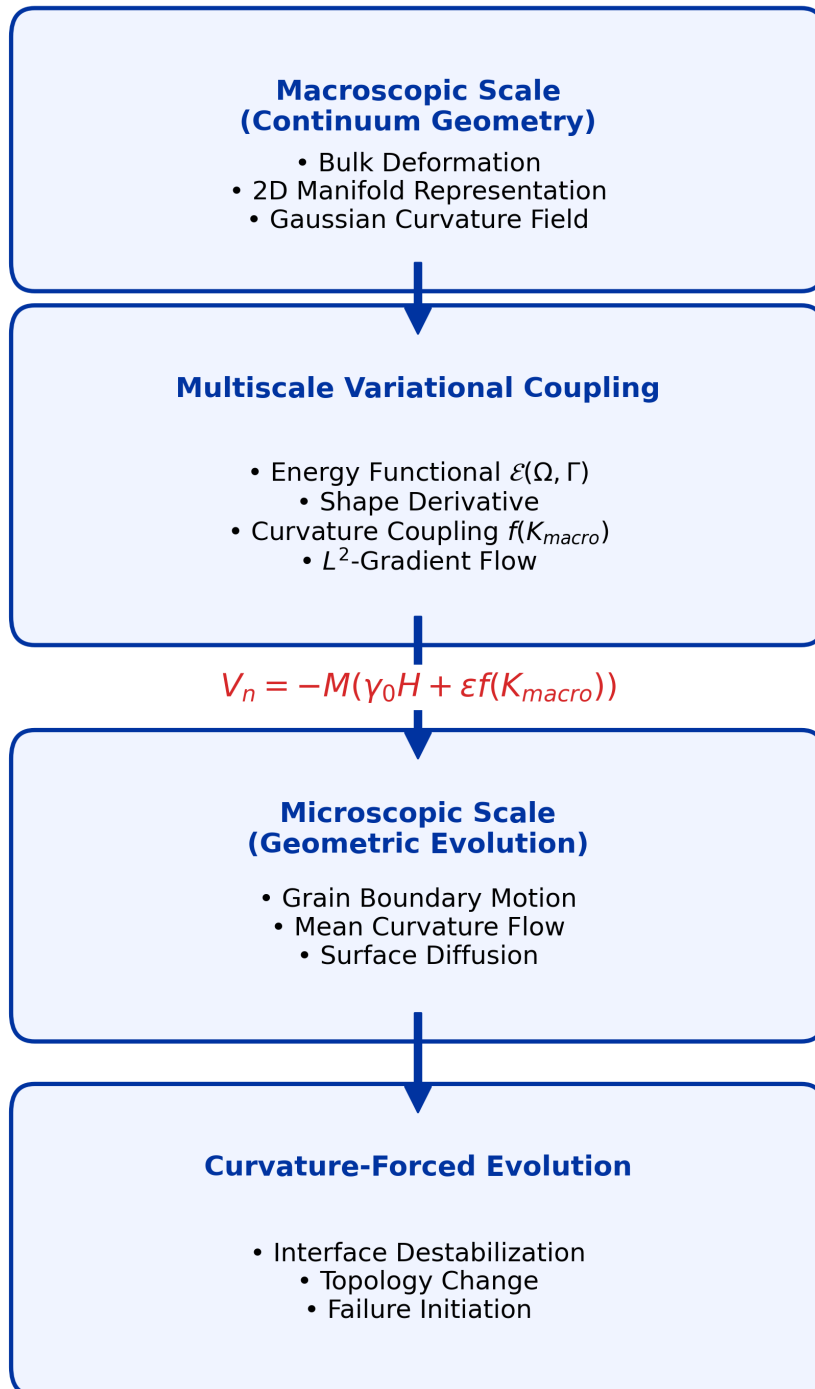


Figure 1: Overall framework of the multiscale geometric PDE model.

## 2 The Physical Object and Continuum Model

This study focuses on the macroscopic deformation of a snow mass resting on a cylindrical guardpipe. Following a drop in temperature below freezing, an initial snow layer and an ice-bonding network were established. Subsequently, a rise in temperature approaching  $0^\circ\text{C}$  induced a decrease in the viscosity of the snow [6, 12]. The emergence of a minor liquid phase within the snowpack further reduced the compressive viscosity coefficient. This warming acted as the environmental factor for the slip and sagging deformation over the guardpipe.

Although snow is a porous structure composed of an ice matrix and pore space, we employ a homogenized continuum approximation to formulate the macroscopic deformation. We consider a snow layer of thickness  $h = 0.1\text{ m}$  on a guardpipe of radius  $R = 0.03\text{ m}$  as a continuum in a cylindrical coordinate system  $(r, \theta, y)$ , as illustrated in Fig. 2. Let the displacement vector be  $\mathbf{u} = (u_r, u_\theta, u_y)$ . The infinitesimal strain tensor components, specifically the circumferential normal strain  $\epsilon_{\theta\theta}$  and the shear strain  $\epsilon_{\theta y}$ , are defined as:

$$\epsilon_{\theta\theta} = \frac{1}{r} \frac{\partial u_\theta}{\partial \theta} + \frac{u_r}{r} \quad (1)$$

$$\epsilon_{\theta y} = \frac{1}{2} \left( \frac{\partial u_\theta}{\partial y} + \frac{1}{r} \frac{\partial u_y}{\partial \theta} \right) \quad (2)$$

The second term  $u_r/r$  in Eq. (1) represents a geometric effect where outward radial displacement causes circumferential stretching.

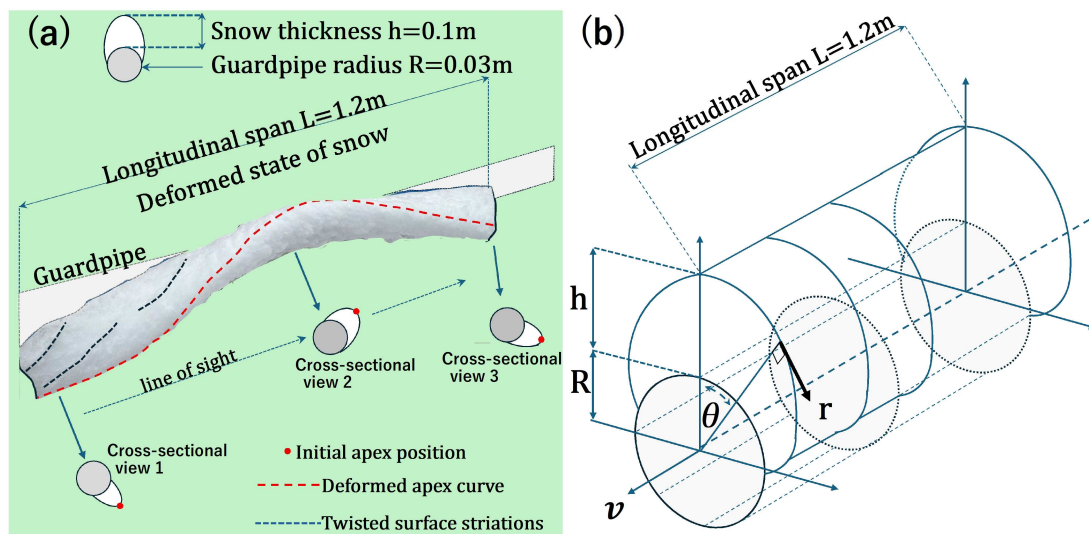


Figure 2: Geometric configuration and coordinate system of the snow layer on the guardpipe. (a) Conceptual illustration of the deformed state of snow, showing the physical dimensions: guardpipe radius  $R = 0.03\text{ m}$ , snow thickness  $h = 0.1\text{ m}$ , and longitudinal span  $L = 1.2\text{ m}$ . (b) Mathematical representation of the continuum. Here,  $r$  represents the radial variable,  $\theta$  is the angular coordinate in the circumferential direction, and  $v$  denotes the longitudinal parameter along the guardpipe.

### 3 Macroscopic Differential Geometric Formulation

To geometrically evaluate the macroscopic strain, we treat the neutral surface of the snow layer (radius  $R_0 = R + h/2 = 0.08$  m) as a two-dimensional manifold (Fig. 2). We denote the angular parameter by  $u$  and the longitudinal parameter along the guardpipe by  $v$  (with an analytical span of  $L$ ). The initial state  $\mathbf{p}_0(u, v)$  is parameterized as:

$$\mathbf{p}_0(u, v) = (R_0 \sin u, v, R_0 \cos u) \quad (3)$$

In surface theory [5], the first fundamental form is computed as the inner products of the tangent vectors:

$$E = \frac{\partial \mathbf{p}}{\partial u} \cdot \frac{\partial \mathbf{p}}{\partial u}, \quad F = \frac{\partial \mathbf{p}}{\partial u} \cdot \frac{\partial \mathbf{p}}{\partial v}, \quad G = \frac{\partial \mathbf{p}}{\partial v} \cdot \frac{\partial \mathbf{p}}{\partial v} \quad (4)$$

The second fundamental form ( $L, M, N$ ) is defined as the inner products of the second-order partial derivatives and the unit normal vector  $\boldsymbol{\nu}(u, v)$ :

$$L = \frac{\partial^2 \mathbf{p}}{\partial u^2} \cdot \boldsymbol{\nu}(u, v), \quad M = \frac{\partial^2 \mathbf{p}}{\partial u \partial v} \cdot \boldsymbol{\nu}(u, v), \quad N = \frac{\partial^2 \mathbf{p}}{\partial v^2} \cdot \boldsymbol{\nu}(u, v) \quad (5)$$

The macroscopic Gaussian curvature  $K_{\text{macro}}$  is given by:

$$K_{\text{macro}} = \frac{LN - M^2}{EG - F^2} \quad (6)$$

In the undeformed initial state,  $N = 0$ , yielding  $K_{\text{macro}} = 0$ .

The decrease in viscosity induces a slip angle  $\alpha(v, t)$  and a downward sagging displacement  $w(u, v, t)$ . The deformed state  $\mathbf{p}(u, v, t)$  is expressed as:

$$\mathbf{p}(u, v, t) = \{R_0 \sin[u - \alpha(v, t)], v, R_0 \cos[u - \alpha(v, t)] - w(u, v, t)\} \quad (7)$$

Calculating the fundamental forms from  $\mathbf{p}(u, v, t)$ , the macroscopic Gaussian curvature  $K_{\text{macro}}$  after deformation is analytically derived as:

$$K_{\text{macro}} = -\frac{\frac{\partial^2 w}{\partial v^2} \cos(u - \alpha)}{R_0 \left\{ 1 + \left( \frac{\partial w}{\partial v} \cos(u - \alpha) \right)^2 \right\}^2} \quad (8)$$

This solution indicates that non-uniform creep deformation with longitudinal deflection ( $\partial^2 w / \partial v^2 \neq 0$ ) causes the manifold to deviate to a nonzero Gaussian curvature field. The emergence of a nonzero Gaussian curvature indicates a geometrically nontrivial deformation of the manifold, which we associate with the accumulation of macroscopic strain energy.

### 4 The Coupled Macroscopic-Microscopic Model via Variational Principle

We establish a theoretical framework using the variational principle to couple the macroscopic deviation of the Gaussian curvature field with the microscopic interfacial evolution. We introduce a parameter  $\epsilon \ll 1$  to characterize the scale separation between the bulk deformation and the interfacial dynamics.

## 4.1 Definition of the Hierarchical Energy Functional

Let  $\Omega \subset \mathbb{R}^3$  be the bulk region and  $\Gamma = \partial\Omega$  be the two-dimensional manifold representing the microscopic interface. We assume that the macroscopic curvature field is transmitted to the microscopic interface through an effective energetic coupling. We define the total energy functional  $\mathcal{E}(\Omega, \Gamma)$  as:

$$\mathcal{E}(\Omega, \Gamma) = \int_{\Gamma} \gamma_0 dA + \epsilon \int_{\Omega} W_{\text{macro}}(K_{\text{macro}}) dV \quad (9)$$

where  $\gamma_0$  is the surface tension, and  $W_{\text{macro}}(K_{\text{macro}})$  is the strain energy density function depending on the macroscopic Gaussian curvature  $K_{\text{macro}}$ .

## 4.2 Shape Derivative and Chemical Potential

Assuming the interface  $\Gamma$  moves with a normal velocity  $V_n = \delta \mathbf{x} \cdot \boldsymbol{\nu}$ , we consider the first variation (shape derivative) of the total energy. The variation of the surface area integral yields the mean curvature  $H$  [5]. For the bulk energy term, its variation with respect to the interface domain  $\Gamma$  introduces a geometric coupling term  $f(K_{\text{macro}})$ , defined as  $f(K_{\text{macro}}) = \frac{\delta}{\delta \Gamma} (\int_{\Omega} W_{\text{macro}}(K_{\text{macro}}) dV)$ . The first variation is therefore obtained as:

$$\delta \mathcal{E} = \int_{\Gamma} (\gamma_0 H + \epsilon f(K_{\text{macro}})) V_n dA \quad (10)$$

The term  $\mu = \gamma_0 H + \epsilon f(K_{\text{macro}})$  represents the chemical potential driving the motion of the interface. This provides a variationally motivated geometric driving term.

## 4.3 Derivation of the Coupled PDE and Mathematical Properties

Treating the evolution as an  $L^2$ -gradient flow, the normal growth velocity  $V_n$  (with mobility  $M$ ) leads to:

$$V_n = -M (\gamma_0 H + \epsilon f(K_{\text{macro}})) \quad (11)$$

Using the identity  $-\Delta_{\gamma} \mathbf{x} = H \boldsymbol{\nu}$ , Eq. (11) can be rewritten as:

$$\frac{\partial \mathbf{x}}{\partial t} = M \gamma_0 \left( -\Delta_{\gamma} \mathbf{x} - \epsilon \frac{f(K_{\text{macro}})}{\gamma_0} \boldsymbol{\nu} \right) \quad (12)$$

At the contact lines with a rigid substrate, we assume a constant contact angle condition governed by Young's equation, and macroscopic failure occurs when the macroscopic shear stress overcomes the microscopic interfacial strength [13].

**Theorem 1 (Local existence).** *Under the assumption that the macroscopic curvature  $K_{\text{macro}}$  is bounded and the geometric coupling term  $f(K_{\text{macro}})$  is locally Lipschitz continuous, the evolution equation (12) falls within the class of quasilinear geometric evolution equations. Thus, local-in-time existence of classical solutions can be established. The proof follows from standard quasilinear parabolic theory.*

In a state where  $K_{\text{macro}} = 0$ , this equation rigorously reduces to the Mean Curvature Flow (MCF). Therefore, the classical MCF appears as the unforced limit of the present model. When non-uniform deformation generates a nonzero Gaussian curvature field, the macroscopic strain energy term affects the smoothing effect of  $-\Delta_{\gamma} \mathbf{x}$ , acting as a mechanism for topological changes (rupture) of the network. Therefore, the proposed model can be viewed as a curvature-forced perturbation of classical mean curvature flow.

## 5 Illustrative Example: Curvature-Forced Topology Change

To conceptually demonstrate the behavior of the proposed theoretical formulation, we present an illustrative computational example for a continuum with a longitudinal span of  $L = 1.2$  m along the guardpipe. Setting  $u = 0$  in the manifold's position vector  $\mathbf{p}(u, v, t)$ , the apex curve is expressed as a space curve  $\mathbf{r}(v)$ :

$$\mathbf{r}(v) = \{-R_0 \sin \alpha(v), v, R_0 \cos \alpha(v) - w(v)\} \quad (13)$$

For this example, the slip angle  $\alpha(v)$  and the sagging displacement  $w(v)$  are represented as quadratic functions to reflect localized deformation near the boundaries:

$$\alpha(v) = \alpha_0 + \alpha_1 \left(\frac{2v}{L}\right)^2 \quad (14)$$

$$w(v) = w_0 + w_1 \left(\frac{2v}{L}\right)^2 \quad (15)$$

The curvature  $\kappa$  of this space curve is calculated as:

$$\kappa = \frac{|\mathbf{r}'(v) \times \mathbf{r}''(v)|}{|\mathbf{r}'(v)|^3} \quad (16)$$

We note that the curve curvature  $\kappa$  is used here as an indicator of the localized geometric distortion. The associated macroscopic Gaussian curvature field  $K_{\text{macro}}$ , which acts as the source of the macroscopic strain energy, is obtained from Eq. (8).

### 5.1 Competition Ratio and the Unforced Limit

To quantitatively evaluate the behavior of the coupled geometric evolution equation, we utilize the dimensionless competition ratio  $R$  between the macroscopic forcing term and the microscopic smoothing term:

$$R = \frac{|\epsilon f(K_{\text{macro}})|}{\gamma_0 |H|} \quad (17)$$

When the macroscopic deformation is negligible ( $K_{\text{macro}} \approx 0$ ), the ratio satisfies  $R < 1$ . This condition implies that the curvature forcing term is weaker than the classical mean-curvature contribution (MCF-dominated regime). The interfacial velocity is then dominated by the mean curvature flow ( $V_n \approx -M\gamma_0 H$ ). In this regime, driven by the Kelvin effect, highly concave inter-particle necks ( $H < 0$ ) act as vapor sinks, causing the interface to grow to minimize the local surface area [2]. This geometric smoothing corresponds to the physical mechanism of microstructural sintering.

### 5.2 Curvature-Forced Topology Change

Figure 3 illustrates the relationship between the localized geometric distortion, the macroscopic Gaussian curvature, and the resulting interfacial velocity. As shown in Fig. 3a, the deformation induces an increase of the curve curvature  $\kappa$  near the boundaries. This localized geometric distortion is associated with the emergence of a nonzero Gaussian curvature field  $|K_{\text{macro}}|$  on the two-dimensional manifold (Fig. 3b).

At these regions, the curvature-forced perturbation term  $\epsilon f(K_{\text{macro}})$  increases. When the competition ratio exceeds unity ( $R > 1$ , Fig. 3c), the curvature-forced term becomes comparable to or larger than the classical smoothing term. As depicted in Fig. 3d, assuming the interface

is locally concave ( $H < 0$ ) corresponding to a sintering neck, this condition significantly modifies the sign and magnitude of the normal velocity  $V_n$ . In this curvature-forced regime, the  $L^2$ -gradient flow may induce interface destabilization and subsequent topology change. The sequence in Fig. 3 provides a conceptual mechanism connecting the macroscopic strain energy accumulation to the initiation of macroscopic failure. The proposed competition ratio  $R$  therefore serves as a geometric indicator for the transition between the MCF-dominated and curvature-dominated regimes.

Furthermore, this theoretical prediction is strongly supported by physical observations. As summarized in Fig. 4, the macroscopic bending deformation of a snow mass demonstrates the curvature-forced destabilization ( $R > 1$ , top row), whereas the interfacial adhesion at the bottom surface highlights the thermodynamic smoothing driven by the Laplace-Beltrami operator ( $R < 1$ , bottom row). This dual mechanism bridges the conceptual gap between continuum deformation and microscopic interface evolution.

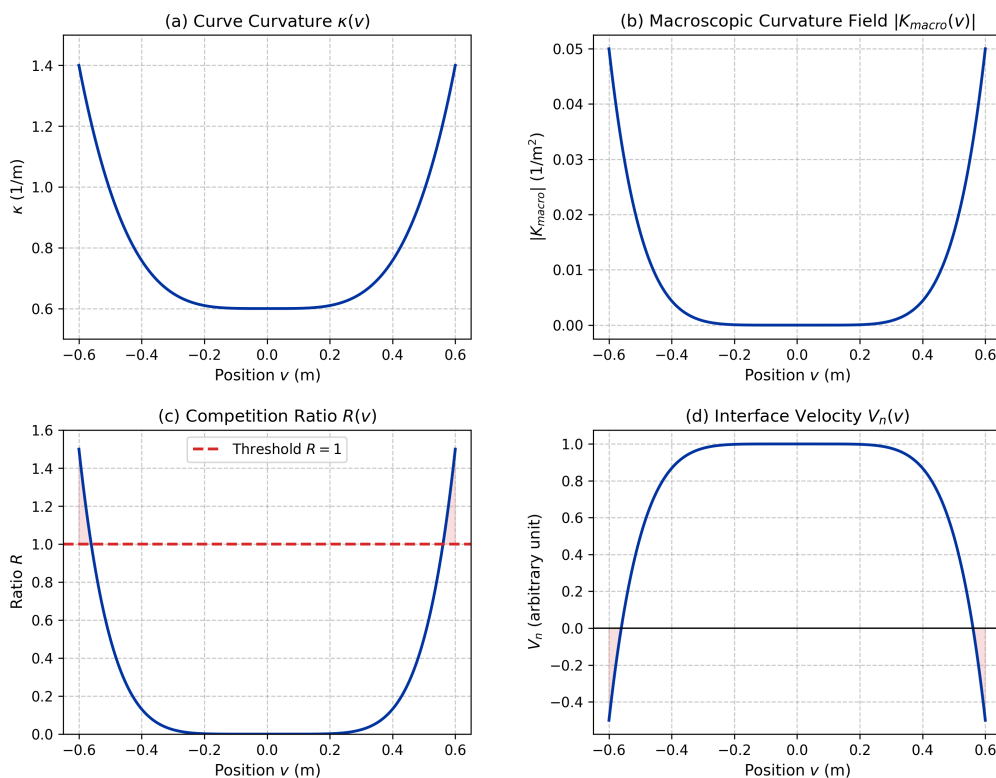


Figure 3: Illustrative example of the proposed curvature-forced geometric evolution model. (a) Curve curvature  $\kappa(v)$ , used as an indicator of localized geometric distortion. (b) Associated macroscopic Gaussian curvature field  $|K_{\text{macro}}(v)|$ . (c) Competition ratio  $R = |\epsilon f(K_{\text{macro}})|/(\gamma_0|H|)$ . Regions with  $R > 1$  correspond to a curvature-dominated regime. (d) Interface velocity  $V_n$ . The interface is assumed to be locally concave ( $H < 0$ ), corresponding to a sintering neck. The sign change of  $V_n$  indicates a transition from mean-curvature-driven smoothing to a curvature-forced destabilization regime.

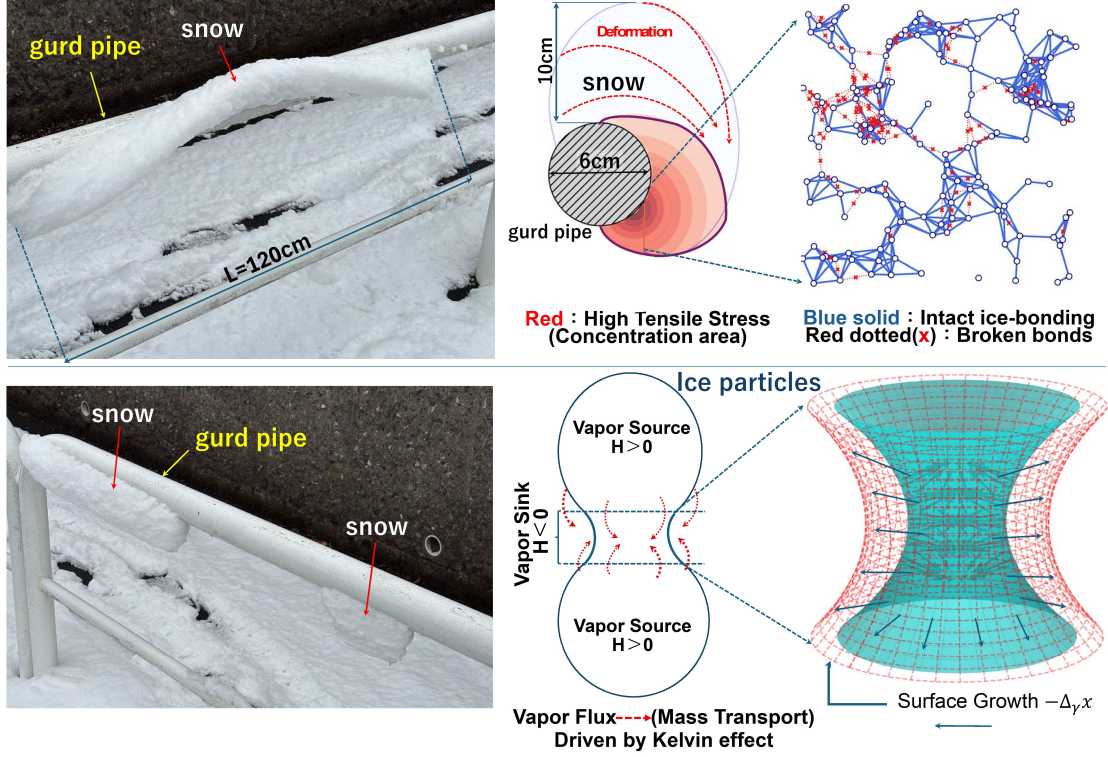


Figure 4: Dual mechanisms of curvature-forced destabilization and surface-tension-driven smoothing in snow deformation. **(Top row)** Macroscopic deformation and microscopic failure. The left photograph shows a snow mass undergoing significant bending on a guardpipe. The corresponding theoretical diagram (right) illustrates how macroscopic tensile stress concentration induces microscopic topology changes, specifically the rupture of the ice-bonding network, in the curvature-dominated regime ( $R > 1$ ). **(Bottom row)** Microscopic interfacial adhesion and smoothing. The left photograph shows snow adhering to the lower surface of the guardpipe, where microscopic ice-bonding resists macroscopic gravitational shear. The theoretical diagram (right) depicts the thermodynamic smoothing mechanism: concave regions ( $H < 0$ ) act as vapor sinks due to the Kelvin effect, driving mass transport and surface growth governed by the Laplace-Beltrami operator ( $-\Delta_\gamma \mathbf{x}$ ) in the mean-curvature-flow (MCF)-dominated regime ( $R < 1$ ).

## 6 Discussion and Concluding Remarks

In this study, we developed a multiscale geometric partial differential equation (PDE) framework to describe the interface evolution of complex materials subjected to macroscopic continuum deformation. The principal contribution of this paper is the derivation of a novel geometric evolution equation that variationally couples the macroscopic curvature field with the microscopic grain boundary motion through a variationally defined energetic formulation.

By introducing a parameter  $\epsilon \ll 1$  to characterize the scale separation, we defined a unified energy functional integrating the microscopic surface free energy and the macroscopic elastic strain energy. The first variation of this functional leads to an  $L^2$ -gradient flow where the normal velocity of the interface is given by  $V_n = -M(\gamma_0 H + \epsilon f(K_{\text{macro}}))$ . This resulting mathematical structure clarifies that the proposed model can be viewed as a curvature-forced perturbation of the classical mean curvature flow (MCF).

To quantitatively evaluate the phase transition between the microstructural smoothing and the macroscopic failure, we introduced the dimensionless competition ratio  $R$ . As demonstrated in the illustrative example of snow deformation, the unforced limit ( $R < 1$ ) corresponds to the MCF-dominated regime, providing a geometric description for the microstructural sintering (ice-bonding). Conversely, a highly non-uniform deformation induces a localized accumulation of macroscopic strain energy, represented by the emergence of a strongly nonzero Gaussian curvature field. When the macroscopic forcing term overwhelms the microscopic smoothing term ( $R > 1$ ), the coupled PDE implies interface destabilization and subsequent topological changes. This theoretical framework successfully bridges the conceptual gap between the macroscopic geometric distortion and the rupture of the microscopic network.

Beyond the illustrative example of snow, the proposed framework provides a general geometric paradigm for multiscale interface evolution in porous and polycrystalline materials subjected to macroscopic deformation. While this study focuses on the theoretical formulation, recent advances in phase-field modeling for complex interface dynamics and snow metamorphism [4, 11, 14] offer promising computational approaches to numerically validate and extend the proposed model. The combination of geometric curvature fields, variational coupling, and interface evolution opens a new avenue for the study of topology change and failure mechanisms in complex materials.

## References

- [1] R L Brown. A volumetric constitutive law for snow based on a neck growth model. *Journal of Applied Physics*, 51(1):161–165, 1980.
- [2] Samuel C Colbeck. Thermodynamics of snow metamorphism due to variations in curvature. *Journal of Glaciology*, 26(94):291–301, 1980.
- [3] Silene Cresseri. *Constitutive modelling of dry granular snow at low strain rates*. PhD thesis, Politecnico di Milano, 2005.
- [4] Thomas U Kaempfer and Mathis Plapp. Phase-field modeling of dry snow metamorphism. *Physical Review E*, 79(3):031502, 2009.
- [5] Miyuki Koiso. Variational problems and curves/surfaces. *Mathematical Sciences*, 62(2):22–29, 2024. (in Japanese).
- [6] Kenji Kojima. Visco-elastic property of snow. *Low Temperature Science, Series A*, 12:1–15, 1954. (in Japanese).

- [7] Edward R LaChapelle. The fundamental processes in conventional avalanche forecasting. *Journal of Glaciology*, 26(94):75–84, 1980.
- [8] Puneet Mahajan and R L Brown. A microstructure-based constitutive law for snow. *Annals of Glaciology*, 18:287–294, 1993.
- [9] David M McClung. The elements of applied avalanche forecasting, part ii: The physical issues and the rules of applied avalanche forecasting. *Natural Hazards*, 26(2):131–158, 2002.
- [10] Malcolm Mellor. A review of basic snow mechanics. In *Proceedings of the Snow Mechanics Symposium, Grindelwald*, pages 251–291, 1974.
- [11] Adrian Moure and Xiaojing Fu. A phase-field model for wet snow metamorphism. *Crystal Growth & Design*, 24(19):7808–7821, 2024.
- [12] Tsuyoshi Ohnishi. A new rheological model for deposited snow. *Seppyo*, 23(6):159–166, 1961. (in Japanese).
- [13] Gianmarco Vallero, Monica Barbero, Fabrizio Barpi, Mauro Borri-Brunetto, Valerio De Biagi, Yoichi Ito, and Satoru Yamaguchi. Experimental study of the shear strength of a snow-mortar interface. *Cold Regions Science and Technology*, 193:103430, 2022.
- [14] Wenqiang Zhang, Armin Shahmardi, Kwing-so Choi, Outi Tammisola, Luca Brandt, and Xuerui Mao. A phase-field method for three-phase flows with icing. *Journal of Computational Physics*, 458:111104, 2022.